Defense Technical Information Center

Compilation Part Notice

ADP011154

TITLE: Active Control of Compressor Surge Using a Real Time Observer

DISTRIBUTION: Approved for public release, distribution unlimited

This paper is part of the following report:

TITLE: Active Control Technology for Enhanced Performance Operational
Capabilities of Military Aircraft, Land Vehicles and Sea Vehicles
[Technologies des systemes a commandes actives pour l'amelioration des
performances operationnelles des aeronefs militaires, des vehicules
terrestres et des vehicules maritimes]

To order the complete compilation report, use: ADA395700

The component part is provided here to allow users access to individually authored sections
of proceedings, annals, symposia, etc. However, the component should be considered within
the context of the overall compilation report and not as a stand-alone technical report.

The following component part numbers comprise the compilation report:
ADP011101 thru ADP011178

Active Control of Compressor Surge Using a Real Time Observer

J.V.R. Prasad[1], Yedidia Neumeier[2], Assaad Krichene[3]
School of Aerospace Engineering
Georgia Institute of Technology, 270 Ferst Drive
Atlanta, GA 30332-0150, USA

Abstract

Approaches for active control of surge in axial and centrifugal compressors are based, for their majority, on sensing them after they occur and then taking appropriate action. On the other hand, some studies in the past have showed that precursors to surge exist in some cases. But very few studies have actually made use of precursors for active control. In this paper we show experimentally that surge precursors exist in centrifugal compressors. Further, we formulate a novel control scheme in which a real time observer is used for on-line identification of magnitude and frequency of dominant precursor waves. The observer outputs feed into a fuzzy logic control scheme, and the identified frequency and amplitude of the precursors are used to actuate a bleed valve and/or a fuel valve for active control of compressor surge. Experimental results demonstrating the viability of the overall scheme are presented.

Introduction

The design and operation of jet engines are faced with many challenges that limit the operating range of those engines. Among those challenges are aerodynamic phenomena that occur in the compression system such as rotating stall and surge. Rotating stall manifests itself as a region of severely reduced flow that rotates at a fraction of the compressor rotational speed and causes a drop in performance. Surge is a pumping oscillation that can cause flameout and engine damage.

Due to the importance of these phenomena, considerable effort in compression system studies has been focused primarily on the design and implementation of active control schemes to ensure stable operation of the compression system over a wide range of operating conditions[1-9]. However, those schemes, in their majority, are based on sensing after those phenomena have occurred and then taking appropriate control action. But the severity of those phenomena and their impact on the engine performance make it highly desirable to have a controller that is able to avoid the operation of the compressor in a region where the compressor is susceptible to those phenomena.

Some studies focused on the identification of precursors for surge and were able to show that such precursors exist for axial compressors and may or may not exist for centrifugal compressors depending on the compressor under consideration[10-17]. However, very little use of precursors was made in the design and implementation of controllers, primarily because of the difficulty associated with on-line identification of such precursors.

In this paper, a previously developed real time observer[18] scheme is used for on-line identification of surge precursors. Then, using the outputs from the real time observer, a fuzzy logic control scheme is synthesized for control of compressor bleed and/or fuel flow to the combustor so as to recover or prevent surge occurrence while maintaining the maximum attainable pressure ratio. The new control scheme is implemented and evaluated on the centrifugal compressor facility in the School of Aerospace Engineering at the Georgia Institute of Technology.

This paper is organized as follows: First, the centrifugal compressor facility is described followed by a brief description of the real time observer scheme used in this study. This is followed by a description of the fuzzy logic control scheme developed in this study. Next, experimental results from the centrifugal compressor facility are presented to illustrate the validity of the overall approach, followed by conclusions and current focus of our research.

Centrifugal Compressor Facility

The primary purpose of the centrifugal compressor rig in the School of Aerospace Engineering at the Georgia Institute of Technology is to provide a laboratory facility for control-oriented studies on surge and rotating stall in centrifugal compressors. Therefore, it is imperative that the rig exhibits these phenomena at reasonable time-scales and yet be compact enough to be housed in one of the bays available in the experimental facility.

The centrifugal compressor rig includes an inlet duct, a single-stage centrifugal compressor, a compressor discharge duct, a special plenum, a burner, an exhaust duct and a throttle. Air enters the system from a conical opening at the tip of the compressor inlet duct for smooth transition of flow from the room inlet duct into the compressor. The inlet duct has a constant diameter of 4 inches (101.6 mm). It is angled and extended from the air inlet duct to the compressor inlet. At the compressor inlet, the duct diameter is slightly reduced to fit the diameter of the compressor impeller. The impeller directs the flow radially outward into the compressor discharge duct that leads directly into the plenum. Heat is generated in the plenum by means of a propane burner. The flow leaves the plenum through the plenum exhaust duct where it has to pass through the throttle (butterfly valve) before it finally reaches the room exhaust duct. The parameters of the compressor are given in Table 1.

The single-spool V-5 supercharger compressor is belt-driven by a 40 HP, 3-phase inverter heavy-duty electric motor. It can be operated at variable speeds from approximately 15,000 rpm to 60,000 rpm without the need to stop and make changes or adjustments. At the maximum speed of 60,000 rpm, the compressor is capable of achieving a pressure ratio of approximately 2.25:1.

Parameter	Value
Compressor Inlet Area	0.003888 m^2
Compressor Exit Area	0.002150 m^2
Compressor Inlet Duct Area	0.008107 m^2
Plenum Inlet Duct Area	0.002027 m^2
Plenum Volume	1 m^3
Plenum Exhaust Duct Area	0.008107 m^2
Compressor Inlet Duct Length (L-shaped)	0.889 m
Plenum Inlet Duct Length	0.3048 m
Plenum Diameter	1.016 m
Plenum Exhaust Duct Length	0.3048 m
Compressor Maximum Speed	60,000 rpm
Compressor Nominal Speed	50,000 rpm

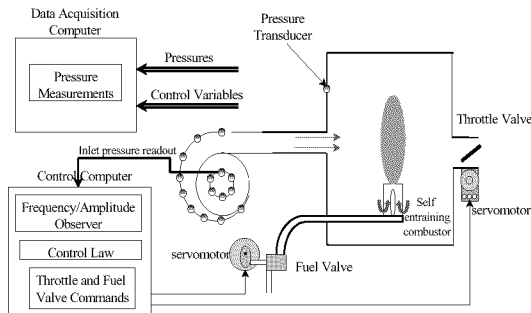Table 1. Centrifugal compressor paprameters.

Figure 1. Schematic of the centrifugal compressor facility.

The plenum is a large metal chamber of 1 m³ in volume. It is made of aluminum that is 3 inches (76.2 mm) thick, and is designed to withstand pressures of up to 400 Psi (27.6 bar). A self-entraining burner is coupled to the plenum at the bottom. The fuel to the burner is controlled by a servo valve. With maximum fuel rate, the burner provides about 15 KW of heat addition. A commercial safety circuit which overrides the operator is used for safe operation of the burner. A quartz window provides visual access to the flame.

The rig is equipped with a throttle actuator and a fuel flow actuator, which are controlled by a computer. Both actuators have a bandwidth of roughly around 10 Hz. The fuel flow actuator consists of a special flow control valve driven by another servomotor. A schematic of the facility together with the control computer and the data acquisition computer is given in Figure 1.

Real Time Observer Scheme

The observer used in this study was previously developed at the Georgia Institute of Technology for identification of combustion instabilities[18]. The observer is capable of real time identification of amplitude, frequency and phase of one or several dominant waves present in a signal. A brief description of the observer and its implementation for the case of identification of one dominant wave is presented here. For a more detailed description, the reader is referred to Ref. 18.

The developed observer assumes that the measured compressor pressure can be expressed in the following Fourier-like series[19]:

$$P_m(t) = \sum_{n=1}^{N} [a_n(t)\sin(\omega_n(t)t) + b_n(t)\cos(\omega_n(t)t)] \tag{1}$$

whose time dependent amplitudes, i.e., $a_n(t)$ and $b_n(t)$, and frequencies $\omega_n(t)$ are as yet unknown and need to be determined by analyzing the measured pressure signal $P_m(t)$. Qualitatively, the determination of these unknowns consists of an iterative solution process that is schematically described in Figure 2[19]. At the start of the calculations, the frequency of the unknown oscillation $\hat{\omega}$ is assumed and substituted into the integrals in Figure 2 and their lower limit of integration. The resulting integrals are then solved for the unknown coefficients $\hat{a}$ and $\hat{b}$. The calculated values of $\hat{a}$, $\hat{b}$ and $\hat{\omega}$ are then substituted into another relationship (not shown in Figure 2) that determines an improved value of the unknown frequency $\hat{\omega}$. The latter is then substituted again into the integrals in Figure 2 to obtain improved values of $\hat{a}$ and $\hat{b}$. This

calculation procedure is repeated until the calculated values of $\hat{a}$, $\hat{b}$ and $\hat{\omega}$ converge to final values. These values of $\hat{a}$, $\hat{b}$ and $\hat{\omega}$ are then used to determine the unknown amplitude, frequency and phase. This solution procedure determines the characteristics of the mode with the largest amplitude first.
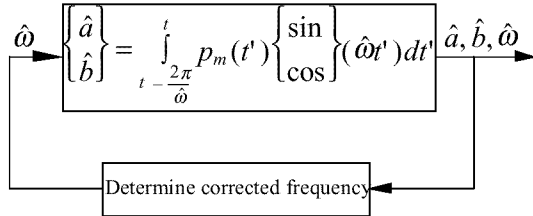
$$\hat{\omega} \rightarrow \begin{Bmatrix} \hat{a} \\ \hat{b} \end{Bmatrix} = \int_{t-\frac{2\pi}{\hat{\omega}}}^{t} p_m(t') \begin{Bmatrix} \sin \\ \cos \end{Bmatrix} (\hat{\omega}t') dt' \rightarrow \hat{a}, \hat{b}, \hat{\omega}$$

Determine corrected frequency

Figure 2. Observer block diagram.

Open Loop Results

The observer described in the previous section was implemented on the control computer of the centrifugal compressor facility. The measured signal and observed frequency and amplitude of the dominant wave for different operating conditions of the compressor are shown in Figures 3, 4 and 5. Figure 3 shows results for the case of low compressor loading, i.e., for the case of nearly full throttle opening. The identified frequency varies randomly in the range of 1 to 2 KHz, indicating a signal dominated by noise. As the loading on the compressor is increased by closing the throttle (see Figure 4), the identified frequency drops to around 100 Hz indicating the presence of dominant waves in the pressure measurements.

As the loading on the compressor is further increased, the compressor surges (see Figure 5), which is evident from large oscillations in pressure. It is also important to note the presence of cursor waves during part of each surge cycle as evidenced by the observed frequency and amplitude.

In order to verify the performance of the observer, an off-line Fast Fourier Transform (FFT) analysis was performed on part of the input signal indicated by two vertical lines in Figure 5. The results are presented in Figure 6. The first plot in Figure 6 shows the inlet pressure variation during the time frame used for performing the FFT analysis. The second plot in Figure 6 is the time dependent identified frequency output from the observer and the third one is a plot of frequency spectrum obtained from FFT analysis over the selected interval. A comparison of the identified frequency output and the FFT results indicates good agreement. Note the peak around 90 HZ in FFT results and the observer identifies the frequency of the dominant wave to be around 90 HZ as well.
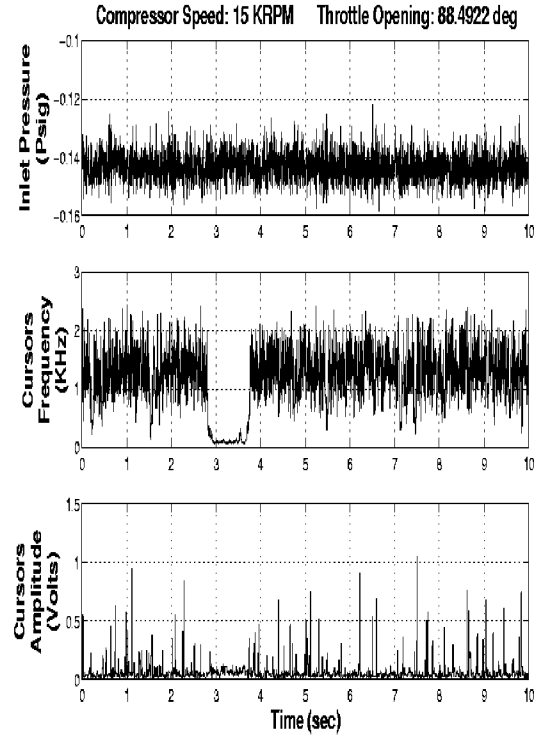

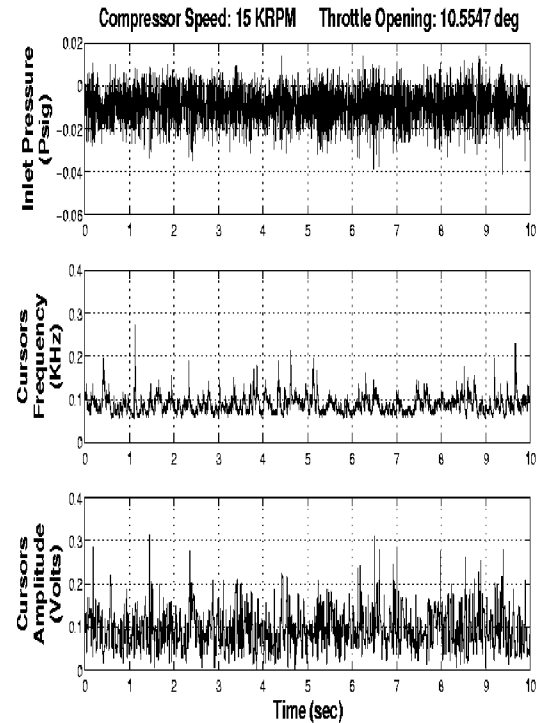Figure 3. Observer performance for the low back pressure case (15,000 rpm)

Figure 4. Observer performance for the high back-pressure case (15,000 rpm)
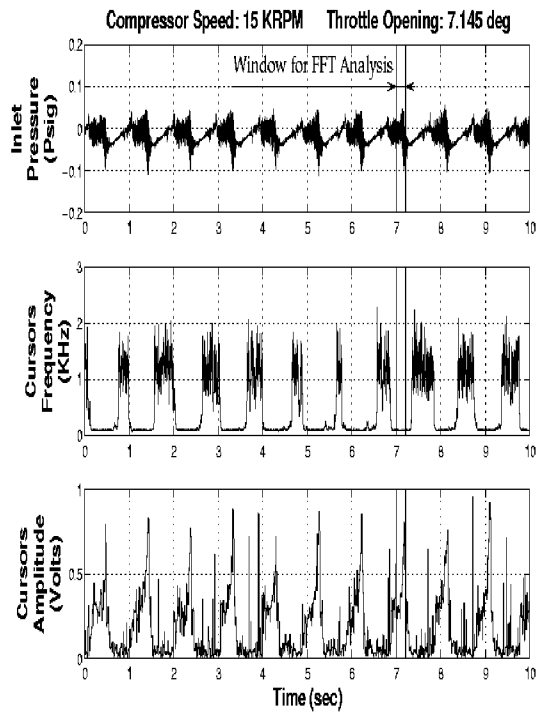
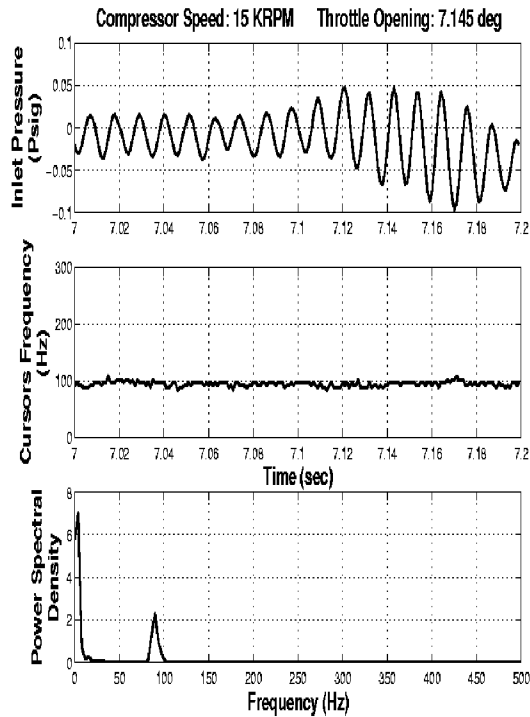Figure 5. Observer performance during uncontrolled surge (15,000 rpm).

Figure 6. Comparison of observer frequency output and FFT results (15,000 RPM)
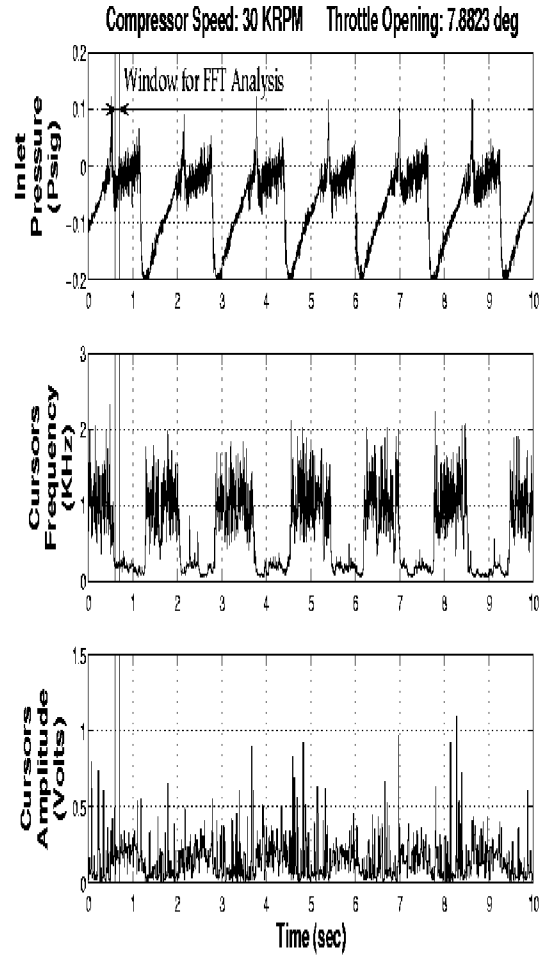
Figure 7. Observer performance during uncontrolled surge (30,000 rpm).

The influence of compressor rpm on the frequency of cursor waves was investigated by repeating the open loop experiments with the compressor rpm set at 20,000, 25,000 and 30,000. Figure 7 shows observer performance during uncontrolled surge with the compressor rpm set at 30,000. Figure 8 is a comparison of the observer frequency output and the results from off-line FFT analysis performed using data over a small time interval (as indicated by the vertical lines in Figure 7). There is a good agreement between the identified frequency from the observer and the FFT results. Note the small peak around 200 Hz in the FFT, which compares well with the average value of observer frequency output of around 200 Hz. Though not shown, similar results were also obtained from experiments conducted at 20,000 rpm and 25,000 rpm. From those results, it was concluded that the precursor frequency varied almost in proportion to the compressor speed and this fact was latter used in closed loop experiments.
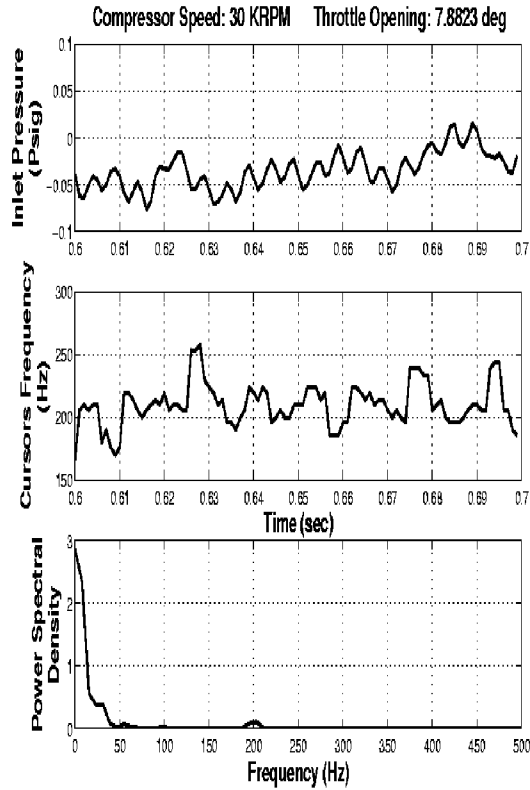
Figure 8. Comparison of observer frequency output and FFT results (30,000 rpm).

Fuzzy Logic Control Scheme

The control scheme uses a pressure transducer located at the inlet face of the compressor. The observer is continuously identifying the frequency and amplitude of dominant waves in the pressure signal. A fuzzy logic scheme is synthesized to make use of the identified frequency and amplitude outputs from the observer and apply appropriate commands to the actuators of a bleed valve or a fuel valve. The objective of the controller is to achieve maximum attainable pressure from the compressor while avoiding surge. It is very important to note that this is achieved with very little knowledge of the compressor characteristic map.

The fuzzy logic scheme consists of a fuzzifier, an inference engine and a defuzzifier. The inputs to the fuzzifier are the frequency distance $|\Delta f|$, and the amplitude difference, ΔA. The frequency distance, $|\Delta f|$, is the absolute value of the difference between the identified frequency and the expected frequency of precursors which depends on compressor rpm; i.e., $|\Delta f| = |$Identified Frequency – Expected Frequency$|$). Likewise, ΔA is the difference between the identified amplitude and a threshold amplitude. These inputs are fuzzified using triangular membership functions with

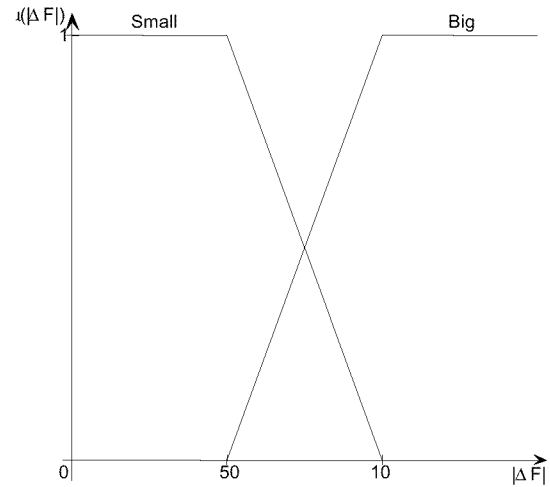two fuzzy sets ("Small" and "Big") for each input (see Figures 9 and 10).

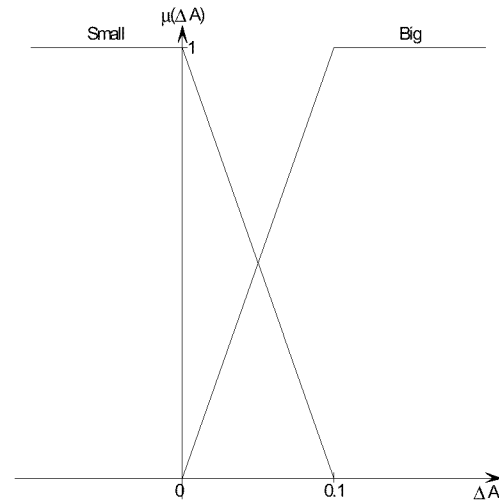Figure 9. Membership functions for identified $|\Delta f|$.

Figure 10. Membership functions for the identified precursor amplitude (ΔA).

ΔA \ $|\Delta f|$	S	B
S	N	N
B	P	AZ

Table 2. Rule base used for the Fuzzy logic Controller.

The fuzzified values of the frequency distance and amplitude difference are then passed through the inference engine consisting of user specified rule-base. The output consists of three fuzzy sets, viz., "Negative (N)", "Approximately Zero (AZ)" and "Positive (P)", (see Table 2).

The fuzzy membership of the output is calculated using Sugeno's product inferencing procedure[20] as follows:

$$x_N = \min\left(\mu_S(\Delta A), \mu_S\left(\left|\Delta f\right|\right)\right) +$$

$$\min\left(\mu_S(\Delta A), \mu_B\left(\left|\Delta f\right|\right)\right)$$

$$x_{AZ} = \min\left(\mu_B(\Delta A), \mu_B\left(\left|\Delta f\right|\right)\right) \quad (2)$$

$$x_P = \min\left(\mu_B(\Delta A), \mu_S\left(\left|\Delta f\right|\right)\right)$$

The crisp value of control is obtained using the weighted average of the fuzzy output values.

$$control = w_N\, x_N + w_{AZ}\, x_{AZ} + w_P\, x_P \quad (3)$$

where w_N, w_{AZ} and w_P are pre-selected output weights.

<u>Closed Loop Results</u>

Closed loop experiments were used to evaluate the performance of the surge controller described in the previous section. Two types of control actuation were considered in this study; viz., bleed valve actuation and fuel valve actuation. In the case of bleed valve actuation, the exit throttle itself was used to emulate a bleed valve. We feel that the fuel control scheme offers inherent advantages such as greater control authority and overheating protection of the turbine.

For each control actuation scheme, two sets of experiments were conducted. In the first set, the performance of the controller for recovery from surge was evaluated. In the second set of experiments, the performance of the controller in avoiding surge was evaluated.

<u>Throttle Control</u>

Figure 11 shows the time dependence of the inlet pressure (which is used as input to the observer), relative plenum pressure rise and throttle position in surge recovery tests. The upper trace in Figure 11 indicates that at large throttle openings, i.e., for low compressor loading, the gage pressure at the inlet is negative indicating that air is flowing into the compressor. Then, as the throttle is closed, this pressure starts to increase which is synonymous to a reduction in the mass flow through the compressor, and this trend continues until the system gets into surge. Note that during parts of surge cycles, the inlet gage pressure is positive indicating flow reversal.

The middle plot in Figure 11 shows that as the throttle is closed, the plenum pressure increases until the system gets into surge at which point the plenum pressure starts oscillating. Note the large decrease in the plenum pressure during surge. Eventually, when the controller is turned on, the surge oscillations diminish and the plenum pressure is recovered to its maximum value.

The lower trace in Figure 11 shows the throttle position commanded by the user and the actual throttle position versus time. When the controller is turned on, although the user commands a more closed position for the throttle, the controller modulates the throttle position just enough to get out of surge and recover the maximum plenum pressure. The throttle modulation would be synonymous to bleed valve modulation in a real engine.

The plots in Figure 12 are similar to those of Figure 11 with the only difference being that in this case, the controller is turned on all the time to demonstrate the surge avoidance capabilities of the controller. In this case, we see that although the commanded position of the throttle goes from a fully open position to a fully closed position, the controller does not allow the actual position of the throttle to go lower than what is necessary to keep the system from surging while maintaining the maximum plenum pressure.
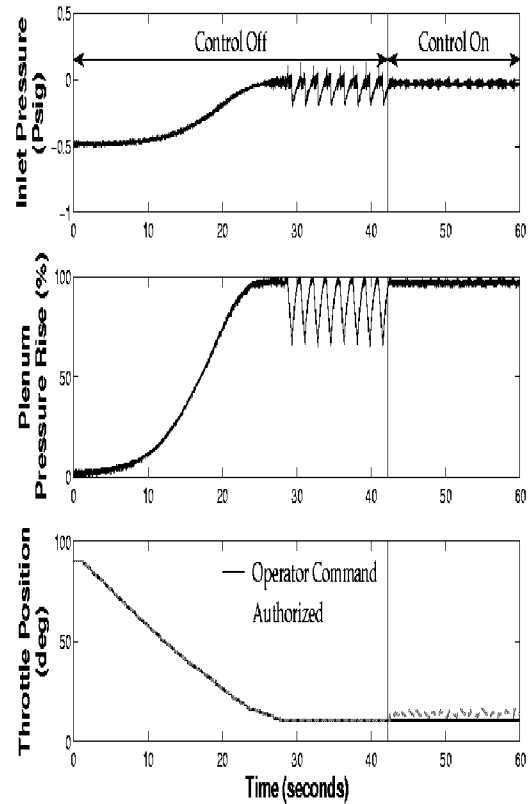

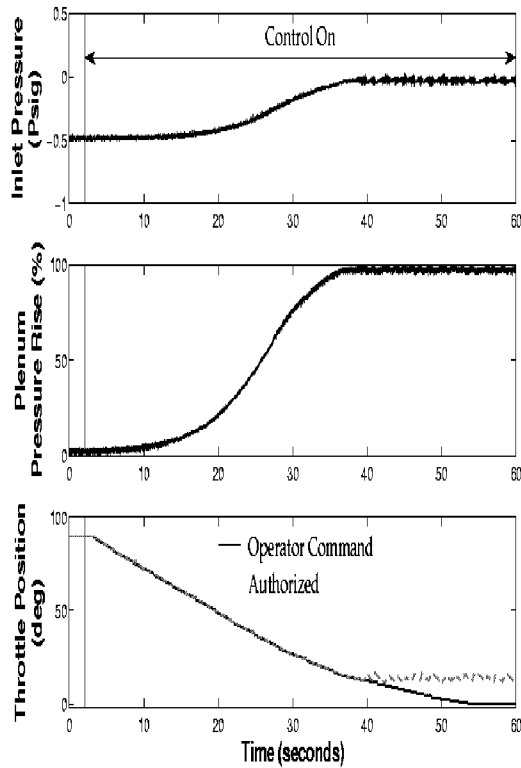Figure 11. Surge recovery using throttle control.
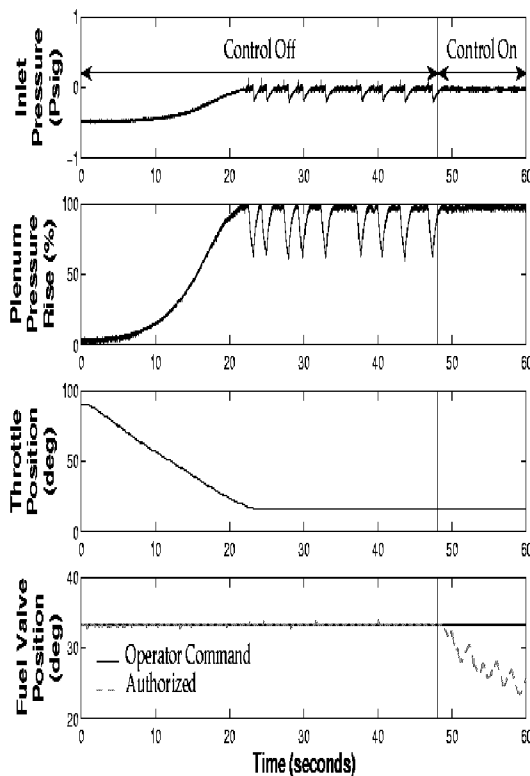
Figure 12. Surge avoidance using throttle control.

Figure 13. Surge recovery using fuel control.

Surge Control Using Fuel Valve

The same controller as before was used with a fuel valve actuation with the only change being that the output of the controller was multiplied by a constant gain to account for differences between control sensitivities associated with the throttle valve actuation and fuel valve actuation.

Figure 13 shows the process of surge recovery using the fuel flow control. The first three traces are similar to those in Figure 11. The additional trace in Figure 13 shows the position of the fuel valve, which is indicative of the fuel flow rate.

Initially, the throttle is open, the fuel valve is fully open and the controller is off. Then, the throttle is closed gradually until the system gets into surge. Once the fuel flow control is turned on, it starts to reduce the fuel flow to recover from surge while maintaining the maximum plenum pressure.
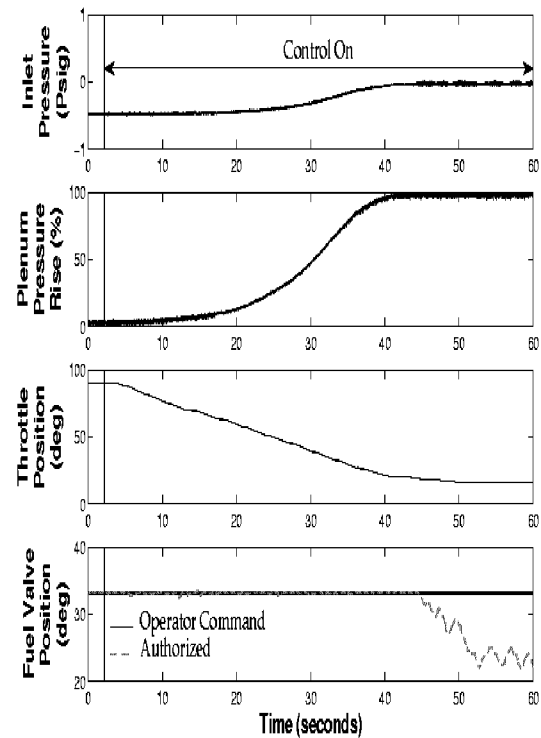

Figure 14. Surge avoidance using fuel Control.

Figure 14 shows similar plots for the surge avoidance case using the fuel valve actuation. In this case, the controller is turned on all the time. The throttle is closed gradually until the system is brought to operate in the surge region while the fuel valve is set at a constant value. Initially, when the system is away from surge, there is no reason for the controller to adjust the fuel flow. As the system gets closer to surge, the fuel flow controller starts reducing the fuel in order to prevent the appearance of surge while maintaining the maximum plenum pressure. In a real

engine, reducing the fuel flow when the compressor gets closer to surge is very desirable since this reduces the temperature, thus protecting the engine components from damage.

Conclusions

An observer previously developed at the Georgia Institute of Technology is used to identify the amplitude and frequency of the dynamic cursors that appear in compressors before and during surge. The amplitude and frequency identified by the observer are used as inputs to a fuzzy logic scheme for active surge control. The surge control scheme has been implemented on the centrifugal compressor facility in the School of Aerospace Engineering at the Georgia Institute of Technology using both throttle valve (that emulates a bleed valve) and fuel valve actuation schemes. Experimental results demonstrate the effectiveness of the surge control scheme developed in this study for both surge recovery and surge avoidance.

Currently work is in progress in providing a detailed understanding of the dynamic cursors and in exploring the potential of the active control schemes developed in this study for full scale compressors.

Acknowledgments

References

1. Day, I. J., "Active Suppression of Stall and Surge in Axial Compressors," *ASME International Gas Turbine and Aeroengine Congress and Exposition, Paper No. 91-GT-403,* June 1991.

2. Epstein, A. H., Ffowcs-Williams, J. E. and Greitzer, E. M., "Active Suppression of Aerodynamic Instabilities in Turbomachines.," *Journal of Propulsion and Power, Volume 5, pages 204 - 211,* March-April 1989.

3. Simon, J. S. and Valavani, L., "A Lyapunov Based Nonlinear Control Scheme for Stabilizing a Basic Compression System Using a Close-Coupled Control Valve," *Proceedings of the 1991 American Control Conference, Volume 3, pages 2398 - 2406,* 1991.

4. Haddad, W. M., Chellaboina, V. S., FauSz, J. L. and Leonessa, A., "Optimal Nonlinear Robust Control for Nonlinear Uncertain Cascade Systems," *Proceedings of the American Control Conference, Volume 1, pages 403 - 407,* 1997.

5. Markopoulos, N., Neumeier, Y., Prasad, J. V. R. and Zinn, B. T., "Active Control of Compressor Rotating Stall Using Linear Amplitude Feedback," *36th Aerospace Sciences Meeting and Exhibit, Reno, NV,* January 12-15, 1998, Paper No. 98-0971.

6. KrstiC, M., "Lyapunov Feedback Design for Stabilization of Stall and Surge in Axial Compressors.," *Nonlinear Dynamics and Controls, ASME Design Engineering Division Publication, Volume 91, pages 73 - 78,* 1996.

7. KrstiC , M., Protz, J. M., Paduano, J. D. and KokotoviC, P. V., "Backstepping Designs for Jet Engine Stall and Surge Control," *Proceedings of the IEEE Conference on Decision and Control,* volume 3, *pages 3049 - 3055,* 1995.

8. Swaminathan, R., Prasad, J.V.R., Neumeier, Y. and Lal, M., "Combined Model and Rule Based Control of Compression System Rotating Stall," *33rd AIAA/ASME/SAE/ASEE Joint Propulsion Conference, Seattle, WA.* July 1997.

9. Krichene, A. and Prasad, J.V.R., "Synthesis of Adaptive Neural Network Based Rotating Stall Controllers for Axial Compressors," *AIAA Guidance, Navigation, and Control Conference and Exhibit, Portland, OR, pages 365 – 373,* Aug. 9-11, 1999.

10. Bright, M. M., Qammar, H. K., Weigl, H. J. and Paduano, J. D., "Stall Precursor Identification In High-Speed Compressor Stages Using Chaotic Time Series Analysis Methods," *Journal of Turbomachinery, Volume 119, No. 3, pages 491 – 499,* July 1997.

11. HÖss, B., Leinhos, D. and Fottner, L., "Stall Inception in the Compressor System of a Turbofan Engine," *Proceedings of the 1998 International Gas Turbine & Aeroengine Congress & Exhibition, Paper No. 98-GT-475,* 1998.

12. Grauer, F., Volgmann, W., Stoff, H. and Breuer, T., "Detection of Precursor Waves Announcing Stall in Two 3-Stage Axial Compressors," *Proceedings of the 1998 International Gas Turbine & Aeroengine Congress & Exhibition, Paper No. 98-GT-520,* 1998.

13. Lawless, P. B., Kim, K. H. and Fleeter, S., "Characterization of Abrupt Rotating Stall Initiation in an Axial Flow Compressor," *Journal of Propulsion and Power, Volume 10, No. 5, pages 709 – 715,* September-October, 1994.

14. Chen, J., Shi, L., Hasemann, H. and Rautenberg, M., "Stall Inception Behavior in a Centrifugal Compressor," *Proceedings of the 1994 International Gas Turbine & Aeroengine Congress & Exhibition, Paper No. 94-GT-159,* 1994.

15. Lawless, P. B. and Fleeter, S., "Rotating Stall Acoustic Signature in a Low Speed Centrifugal Compressor: Part 1 - Vaneless Diffuser," *Proceedings of the 1993 International Gas Turbine & Aeroengine Congress & Exhibition, Paper No. 93-GT-297,* 1993.

16. Lawless, P. B. and Fleeter, S., "Rotating Stall Acoustic Signature in a Low Speed Centrifugal Compressor: Part 2 - Vaned Diffuser," *Proceedings of the 1993 International Gas Turbine & Aeroengine Congress & Exhibition, Paper No. 93-GT-254,* 1993.

17. Inoue, M., Kuroumaru, M., Iwamoto, T. and Ando, Y., "Detection of a Rotating Stall Precursor in Isolated Axial Flow Compressor Rotors," *Journal of Turbomachinery, Volume 113, No. 2, pages 281 - 289,* April 1991.

18. Neumeier, Y., Markopoulos, N. and Zinn, B. T., "A Procedure for Real-Time Decomposition, Observation and Prediction for Active Control of Combustion Instabilities," *Presented at the IEEE Conference on Control Applications, Hartford CT,* October 5-7, 1997, Paper No. 97-318.

19. Neumeier, Y. and Znn, B. T., "Active Control of Combustion Instabilities using Real Time Identification of Unstable Combustor Modes," Proceedings of the 4th IEEE Conference on Control Applications, Albany, NY, September 28-29, 1995.

20. Driankov, D., Hellendoorn, H. and Reinfrank, M.: An Introduction to Fuzzy Logic Control, Springer-Verlag, 1991.

PAPER -11, J. Prasad

Question (F. Grauer, Germany)
Was the detector influenced by the blade passing frequencies?

Reply
No, the observer could be selected to operate over a range of frequencies, thus eliminating other frequencies.

Question (F. Grauer, Germany)
Do you expect your fuel controller to be slow, as was found from another study?

Reply
The bandwidth of the fuel actuator we have used is 10 Hz. We believe similar results could be expected from full scale experiments.